Active modulation of plasmonic signal with a subwavelength metal/nonlinear dielectric material/metal structure

Xiaolei Wang (王小蕾)[1], Pei Wang (王　沛)[1*], Chunchong Chen (陈春翀)[1], Junxue Chen (陈俊学)[1], Yonghua Lu (鲁拥华)[1], Hai Ming (明　海)[1], and Qiwen Zhan (詹其文)[2]

[1]*Department of Physics, Anhui Key Laboratory of Optoelectronic Science and Technology, University of Science and Technology of China, Hefei 230026, China*

[2]*Electro-Optics Graduate Program, University of Dayton, 300 College Park, Dayton, OH 45469, USA*

[*]*E-mail: wangpei@ustc.edu.cn*

Received September 29, 2009

Light propagation through a metal/nonlinear dielectric material/metal (M-NL-M) structure is numerically studied. The design parameters of the M-NL-M structure are found with the waveguide theory so that the structure only supports the symmetric surface plasmon polaritons (SPP(0)) mode and the antisymmetric surface plasmon polaritons (SPP(1)) mode. The coupling between the two modes within the M-NL-M structure is exploited. Through controlling the propagation constants of the two modes with the intensity-dependent dielectric constant of the nonlinear Kerr material, an effective all-optical control of plasmonic signal modulator can be realized with this M-NL-M structure.

OCIS codes: 120.4570, 190.3270, 240.6680.
doi: 10.3788/COL20100806.0584.

Plasmonics is considered to be a very promising area for new devices and the miniaturization of photonic circuits at nanoscale[1]. Currently, the control of the path of surface plasmon polaritons (SPP) is realized with passive subwavelength metal structures[2−5]. In order to achieve functional SPP circuits, active devices is necessary[5]. Recently, the active control of plasmonic signals by implementing electro-optic[6], all-optical[7−9], and thermo-optic modulations[10] and gain mechanisms in plasmonic structures have been reported. Among the various possibilities, fast all-optical control is the most attractive approach[7,8,11,12]. Compared with those usual dielectric all-optical devices based on various types of optical nonlinearities, these new nonlinear optical devices based on subwavelength metal structures have the advantages of smaller sizes and stronger nonlinear effects enhanced by SPP in the metal structures.

In this letter, we propose new active plasmonic devices using a thin layer of nonlinear optical material sandwiched between two layers of metal films with metal/nonlinear dielectric material/metal (M-NL-M) structure. This structure is similar to that proposed in Ref. [13]. However, the light flow in those structures in Ref. [13] is predetermined and cannot be readily modulated during operation, while our structure is an all-optical plasmonic switching that can actively modulate light and possess some advantages of fast response, low threshold, and easy integration. At low incident optical power, the M-NL-M structure can be considered as metal-dielectric-metal (MDM) structure. The parameters of M-NL-M structure can be designed with waveguide theory such that the structure only supports the symmetric SPP (SPP(0)) mode and the antisymmetric SPP (SPP(1)) mode. Coupling of these two distinct modes in the MDM structure will give rise to coherent propagation of energy along the interface of the metal and dielectric, leading to a zigzag path of optical flow power along the slit[13]. Nonlinear optical materials with fast response time and large nonlinear coefficient can be chosen for fast all-optical control[14,15]. Our modulation is based on adjusting the difference between the propagation constants of SPP(0) and SPP(1) by changing the refractive index of the nonlinear Kerr material with light, which is applied to control the distribution of coherent energy. In this letter, we reveal this active signal control mechanism and demonstrate the effect using nonlinear two-dimensional finite difference time domain (2D-FDTD) numerical simulation.

The proposed M-NL-M structure is illustrated in Fig. 1. In this structure, a single slit's filled with nonlinear Kerr optical material in a thick metal film. Silver is chosen to be the metal. The slit width is d, and the slit length is L. $\varepsilon_{\rm all} = \varepsilon_{\rm e} + \varepsilon_{\rm nl}$ is the dielectric constant of the nonlinear optical material in the slit, where $\varepsilon_{\rm e}$ is the linear part and $\varepsilon_{\rm nl}$ is the nonlinear part, and $\varepsilon_{\rm m}$ is the dielectric constant of Ag. For the M-NL-M structure, the optical property depends on the electric field intensity. At the low electric field intensity, the M-NL-M structure can be treated as a MDM structure. In the MDM structure, the field components can be expressed as $\boldsymbol{H}_y = H_y(x)\boldsymbol{e}_y \exp(\mathrm{i}\beta z)$ and $\boldsymbol{E} = [E_x\boldsymbol{e}_x + E_z\boldsymbol{e}_z]\exp(\mathrm{i}\beta z)$ for transverse magnetic (TM) mode, where β is the propagation constant along the z axis, $\boldsymbol{e}_x, \boldsymbol{e}_y$, and $\boldsymbol{e}_z$, are unit vectors along the x, y, and z directions, respectively. Maxwell's equation for TM modes can be written as

$$\begin{aligned}
\frac{\mathrm{d}E_z}{\mathrm{d}x} &= \mathrm{i}\beta E_x - \mathrm{i}\omega\mu_0 H_y,\\
\frac{\mathrm{d}H_y}{\mathrm{d}x} &= -\mathrm{i}\omega\varepsilon_0\varepsilon E_z,\\
\beta H_y &= \omega\varepsilon_0\varepsilon E_x,
\end{aligned} \tag{1}$$

where ε_0 and μ_0 are the free space permittivity and permeability, respectively.

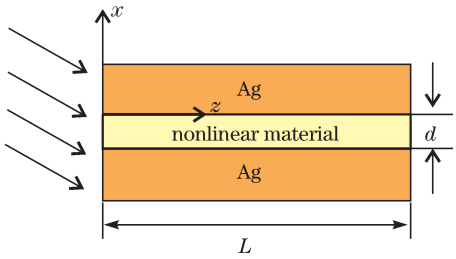

Fig. 1. Schematic layout of the M-NL-M structure. The refractive index of the material which is surrounding the device is 1.

The variation of dielectric constant of the structure takes the following form:

$$\varepsilon = \begin{cases} \varepsilon_d, -d < x < 0 \\ \varepsilon_{\rm m}, x > 0, x < -d. \end{cases} \quad (2)$$

Applying the boundary conditions of continuity of the field components H_y and E_z at the interface between the metal and the nonlinear dielectric, we can derive the dispersion relation for the TM modes in the slit as[16]

$$\kappa_{\rm d} d = m\pi + 2\arctan(\varepsilon_{\rm d}\alpha_{\rm m}/\varepsilon_{\rm m}\kappa_{\rm d}), \quad (3)$$

where $\kappa_{\rm d} = (\boldsymbol{k}_0^2\varepsilon_{\rm d} - \beta^2)^{1/2}$, $\alpha_{\rm m} = (\beta^2 - \boldsymbol{k}_0^2\varepsilon_{\rm m})^{1/2}$, and $\boldsymbol{k}_0$ is the free space wave vector of light. From Eq. (3), we can derive the dispersion relation for $m = 0$ and $m = 1$ modes. Considering $\varepsilon_{\rm m} < 0$, the dispersion relation for $m = 0$ mode has solution only when $\beta/\boldsymbol{k}_0 > \sqrt{\varepsilon_{\rm d}}$, so the dispersion relation for $m = 0$ mode changes into

$$\tanh(\alpha_{\rm d} d/2) = -\varepsilon_{\rm d}\alpha_{\rm m}/\varepsilon_{\rm m}\alpha_{\rm d}, \quad (4)$$

where $\alpha_{\rm d} = (\beta^2 - \boldsymbol{k}_0^2\varepsilon_{\rm d})^{1/2}$. According to Eqs. (1) and Eqs. (4), $m = 0$ mode has no cut-off width, the magnetic field distribution of this mode is symmetric in the core and exponentially decays away from the interfaces (Fig. 2), which is the symmetric SPP mode designated as SPP(0), so in MDM structure, $m = 0$ mode is SPP(0). For $m = 1$ mode, the dispersion relation is

$$\begin{aligned} \kappa_{\rm d} d &= \pi + 2\arctan(\varepsilon_{\rm d}\alpha_{\rm m}/\varepsilon_{\rm m}\kappa_{\rm d}) \\ &= 2\arctan(-\varepsilon_{\rm m}\kappa_{\rm d}/\varepsilon_{\rm d}\alpha_{\rm m}). \end{aligned} \quad (5)$$

Equations (1) and (5) indicate that the magnetic field distribution of the mode in the core is antisymmetry, so $m = 1$ is the antisymmetric mode. According to Eq. (5), it has solution when $0 < \beta/\boldsymbol{k}_0 < \sqrt{\varepsilon_{\rm d}}$ and $\beta/\boldsymbol{k}_0 > \sqrt{\varepsilon_{\rm d}}$, so $m = 1$ mode has two forms and we designate it as SPP(1). Above analysis means that the antisymmetric SPP(1) mode has evolution progress, as shown in Fig. 3.

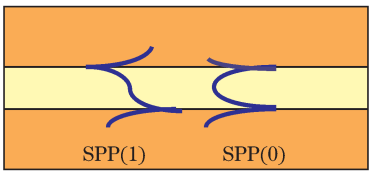

Fig. 2. Magnetic field distributions of SPP(0) and SPP(1) modes.

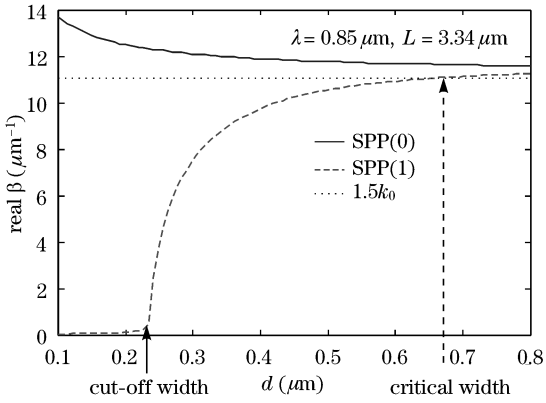

Fig. 3. Real part of propagation constant β_i $(i = 0, 1)$ as a function of the width of the nonlinear optical material slit.

Figure 3 shows the relationship between the real part of propagation constants of these two modes β_i $(i = 0, 1)$ and the width of metal slit d with $\lambda = 850$ nm, $L = 3.34$ μm, and $n_0 = 1.5$. The dotted line represents the wave vector in bulk dielectric with $n_0 = 1.5$, while the solid line represents the SPP(0) mode that has no cut-off width. The dashed line represents the evolution progress of the SPP(1) mode. Firstly, it is cut-off, then the propagation constants along the interface (β) is smaller than wave vector $(\boldsymbol{k}_0\sqrt{\varepsilon_{\rm d}})$ in dielectric, i.e., $0 < \beta/\boldsymbol{k}_0 < \sqrt{\varepsilon_{\rm d}}$ when the slit width increases to ~ 0.236 μm, which is cut-off width, while after the slit width increases to critical width 0.668 μm, the propagation constants along the interface is larger than the wave vector $(\boldsymbol{k}_0\sqrt{\varepsilon_{\rm d}})$ in dielectric, i.e., $\beta/\boldsymbol{k}_0 > \sqrt{\varepsilon_{\rm d}}$.

When the symmetric $m = 0$ and antisymmetric $m = 1$ modes are both excited, they will couple to each other in the slit. The differences of losses of the two modes are not significant at the incident light with the wavelength of 850 nm, so we can assume that these two modes have the same losses. Consequently, these two modes can be expressed as $E_{\rm SPP(0)} = S(0)\exp(\mathrm{i}\beta_0 z)\exp(-\alpha z)$ and $E_{\rm WG(1)} = AS(1)\exp(\mathrm{i}\beta_1 z)\exp(-\alpha z)$, where α is the transmission loss constant, $S(0)$ is the electric field amplitudes of SPP(0) mode, while $AS(1)$ is the electric field amplitudes of SPP(1) modes. The coupling of these two modes leads to a zigzag distribution of light intensity which can be described as[13]

$$\begin{aligned} I(x, z) =& [S(0)]^2 + [AS(1)]^2 + 2[S(0)][AS(1)] \\ & \cos[\Delta\beta z]\exp(-\alpha z), \end{aligned} \quad (6)$$

where $\Delta\beta$ is the difference between the propagation constants of $m = 0$ and $m = 1$ modes along the z axis. When L is fixed, $\Delta\beta$ determines the distribution of coherent light intensity. It shows that the coupling energy transfers from one channel (interface of metal/nonlinear medium) to the other channel periodically with the period given by the coupling length $L_{\rm c} = \pi/\Delta\beta$. When an appropriate slit length is chosen and fixed, light radiates from single channel of the slit, similar to the structure proposed in Ref. [13], where a nanometer light source with high spatial resolution can be realized. If the slit length is fixed, the channel from which the light radiates can be controlled by adjusting $\Delta\beta$. According to Eqs. (4) and (5), $\Delta\beta$ depends on the dielectric constant of

the material in the slit when the wavelength and width of the slit are fixed. If the slit is filled with nonlinear optical material, we can actively control $\Delta\beta$ to modulate the channel from which light radiates. For better sensitivity, large value of $\Delta\beta(|E|^2)$ should be chosen, which requires appropriate d value derived in the case of weak light. According to Fig. 3, we choose $d = 0.25$ μm for large value of $\Delta\beta$, such that there only exist SPP(0) and SPP(1) modes when the structure is irradiated by TM incident light. So we study the coupling between SPP(0) and SPP(1) modes. The distribution of magnetic field of these two modes is shown in Fig. 2.

The Drude dispersion model is applied to describe the metal section (the complex dielectric constant for Ag film at 850 nm is –32.21658+1.726112i). In the proposed M-NL-M structure, most of the light intensity is concentrated in the nonlinear dielectric layer. Thus the nonlinearity of silver is not considered here, even though it is much higher than the nonlinearity of the nonlinear dielectric. A nonlinear 2D-FDTD method is used to simulate the modulating properties of the M-NL-M structure. Recently, the nonlinear optical medium with high third-order nonlinear susceptibility ($\chi^{(3)} - 10^{-6}$esu) has been reported[14]. For our simulation, we choose Au:SiO_2[17,18] as the nonlinear material with $\chi^{(3)} = 1.4 \times 10^{-7}$esu $\approx 10^{-15}$ m^2/V^2.

In order to excite the antisymmetric mode SPP(1), the structure should be illuminated by TM-polarized plane wave at an oblique angle. To obtain the highest modulation contrast means complete transfer of light from one interface to the other, the amplitudes of the SPP(0) and SPP(1) modes should be approximately equal, which are controlled by the incident face of the structure and the incident angle. This can be obtained by varying the incident angle to adjust the coupling into these two modes for a fixed structure. Figure 4 shows the relative power at various angles of incident angle θ with $d = 0.25$ μm and $L = 3.34$ μm. The incident light is a TM-polarized plane wave. The relative power is defined as the peak power on the top side over the power on the opposite side. From it, we can see that when the structure is illuminated by plane wave with the oblique incident angle of 36.5°, most of the light radiates from one side of the slit. The highest modulation contrast is obtained under this condition.

Figure 5 shows the FDTD simulation of the time-average power distribution of light switching with different power densities in the M-NL-M structure with $L = 3.34$ μm at the oblique incident angle of 36.5°,

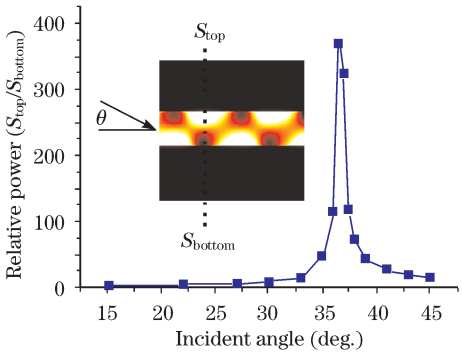

Fig. 4. Relative powers at various incident angles.

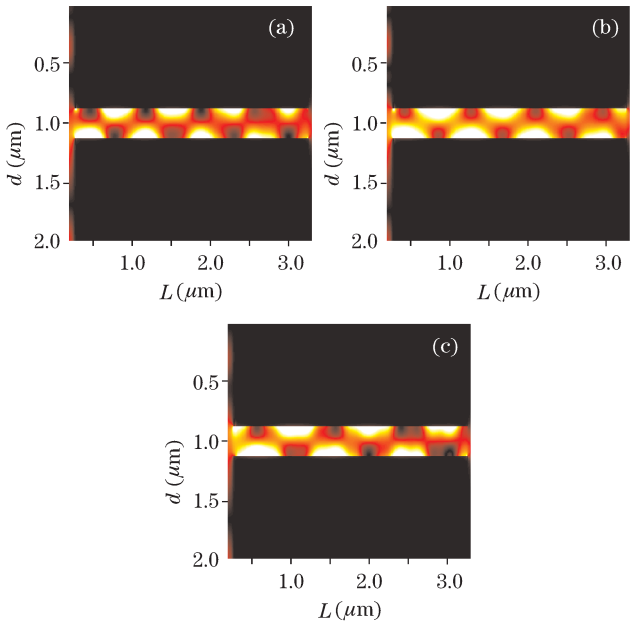

Fig. 5. Nonlinear 2D-FDTD simulation of the time-averaged power distribution of M-NL-M structure. A TM-polarized plane wave illuminates the structure at the oblique angle of 36.5°. The power densities of the incident light are (a) 0.25 MW/cm^2, (b) 56.25 MW/cm^2, and (c) 95 MW/cm^2. d = 0.25 μm, $L = 3.34$ μm.

the linear dielectric constant of nonlinear optical medium is $n_0 = 1.5$, and other parameters are the same as the simulation above. In Fig. 5(a), the light radiates from the bottom interface when $P = 0.25$ MW/cm^2; however, it will switch to the top interface with $P = 56.25$ MW/cm^2, as shown in Fig. 5(b). The phenomenon of switching is consistent with our analysis mentioned above. According to the dispersion relationship given by Eqs. (3) and (4), when the incident light power increases, $\Delta\beta$ decreases and L_c increases, leading to the switching of the channels from which light radiates. Our analysis also predicts that if the power of the incident light continues to increase, L_c keeps increasing as well and the light radiation switches back to the bottom channel again eventually. This result is shown in Fig. 5(c) with a power of $P =$ 95 MW/cm^2. As shown in Fig. 5, the M-NL-M structure can manipulate the transmitted light with different powers of incident light efficiently with low power. If a proper grating structure is fabricated at the output end for each channel, the power flow of each channel can be coupled out into the optical propagation modes out of the waveguide. This proposed structure, which combines all-optical switching and SPPs, can work not only as a simple dual-channel optical router but also possible as unit integrated with surface-plasmon-based photonic circuits to realize the functions of light generation, channeling, switching, and modulation on a metallic chip.

In conclusion, we propose and numericaly demonstrate a concept for the active plasmonics that exploits nanoscale M-NL-M structure. Coupling between SPP(0) and SPP(1) modes can be used to effectively control the light signals. Its mechanism is based on the intensity-dependent behaviors of the propagation constants of two modes by implementing the nonlinear Kerr material. For ultrafast and ultrasensitive optical modulation, the non-

linear Kerr material with large third-order nonlinear susceptibility and ultrafast response is necessary. Owing to the excitation of the SPPs, the M-NL-M structure shows great advantages of lower incident light intensity requirement. The proposed device can be used as a multiport optical switch/router. These results cannot only improve the design of active plasmonic devices, but also are helpful for analyzing the nonlinear phenomenon in subwavelengh M-NL-M array structure[19].

This work was supported by the National Key Basic Research Program of China (No. 2006CB302905), the Key Program of National Natural Science Foundation of China (No. 60736037), the National Natural Science Foundation of China (Nos. 10704070 and 60977019), and the Science and Technological Fund of Anhui Province for Outstanding Youth (No. 08040106805).

References

1. W. L. Barnes, A. Dereux, and T. W. Ebbesen, Nature **424,** 824 (2003).
2. S. I. Bozhevolnyi, V. S. Volkov, E. Devaux, J.-Y. Laluet, and T. W. Ebbesen, Nature **440,** 508 (2006)
3. A. Hohenau, J. R. Krenn, A. L. Stepanov, A. Drezet, H. Ditlbacher, B. Sreinberger, A. Leitner, and F. R. Aussenegg, Opt. Lett. **30,** 893 (2005).
4. S. A. Maier, M. L. Brongersma, P. G. Kik, S. Meotzer, A. A. G. Requicha, and H. A. Atwater, Adv. Mater. **13,** 1501 (2001).
5. E. Ozbay, Science **311,** 189 (2006).
6. S. W. Liu and M. Xiao, Appl. Phys. Lett. **88,** 143512 (2006).
7. G. A. Wurtz, R. Pollard, and A. V. Zayats, Phys. Rev. Lett. **97,** 057402 (2006).
8. A. V. Krasavin, K. F. MacDonald, N. I. Zheludev, and A. V. Zayats, Appl. Phys. Lett. **85,** 3369 (2004)
9. K.-S. Lee, T.-S. Lee, W.-M. Kim, S. Cho, and S. Lee, Appl. Phys. Lett **91,** 141905 (2007).
10. T. Nikolajsen, K. Leosson, and S. I. Bozhevolnyi, Appl. Phys. Lett. **85,** 5833 (2004).
11. I. I. Smolyaninov, Phys. Rev. Lett. **94,** 057403 (2005).
12. C. Min, P. Wang, X. Jiao, Y. Deng, and H. Ming, Opt. Express **15,** 9541 (2007).
13. P.-K. Wei, Y.-C. Huang, C.-C. Chieng, F.-G. Tseng, and W. Fann, Opt. Express **13,** 10784 (2005).
14. H. B. Liao, R. F. Xiao, J. S. Fu, P. Yu, G. K. L. Wong, and P. Sheng, Appl. Phys. Lett. **70,** 1 (1997).
15. W. Wang, G. Yang, Z. Chen, Y. Zhou, H. Lu, and G. Yang, J. Appl. Phys. **92,** 7242 (2002).
16. S. A. Maier, *Plasmonics: Fundamentals and Application* (Springer, Berlin 2007)
17. K. Fukumi, A. Chayahara, K. Kadono, T. Sakaguchi, Y. Horino, M. Miya, K. Fujii, J. Hayakawa, and M. Satou, Jpn. J. Appl. Phys. **30,** L742 (1991).
18. I. Tanahashi, Y. Manabe, T. Tohda, S. Sasaki, and A. Nakamura, J. Appl. Phys. **79,** 1244 (1996).
19. Y. Liu, G. Bartal, D. A. Genov, and X. Zhang, Phys. Rev. Lett. **99,** 153901 (2007).